PHYSICAL REVIEW B VOLUME 40, NUMBER 1 1 JULY 1989

Theory of the magnetic phase diagram and magnetostriction of $FeGe_2$

V. V. Tarasenko
Institute of Radio Engineering and Electronics, Academy of Sciences of the U.S.S.R., Moscow, 103907 Union of Soviet Socialist Republics

V. Pluzhnikov
Physico-Technical Institute of Low Temperatures, Academy of Sciences of the UkSSR, Kharkov, 130164 Union of Soviet Socialist Republics

E. Fawcett
Physics Department and Scarborough College, University of Toronto, Toronto, Canada M5S 1A7

(Received 27 February 1989)

A Landau model based on the competition between quadratic and quartic exchange among moments in the four-sublattice structure of $FeGe_2$ has been used to derive an expression for the free energy, and hence to determine the boundaries of the homogeneous antiferromagnetic (AF) phases in the phase diagram. Two types of AF spiral structure of different symmetry are found. The transverse AF spiral phase exists in comparatively small magnetic fields, $H < H_p \approx H_e(a_o q_c)^2$ (H_e is the exchange field, q_c the spiral wave vector, and a_o the lattice constant), while the longitudinal AF spiral phase exists in stronger magnetic fields up to $H_t \approx H_e a_o q_c$. The phase transition between these two AF spiral structures in the field-temperature phase diagram is first order. The temperature dependence of the wave vector of the spiral structure in the absence of magnetic field is also determined, and the results of magnetostriction experiments are explained.

I. INTRODUCTION

The magnetic properties of $FeGe_2$ have long been the subject of experimental study and theoretical speculation. Experimental studies of the temperature dependence of the resistivity, thermal expansivity, specific-heat and magnetic susceptibility,[1-3] ultrasonic attenuation,[4,5] magnetostriction,[6] and neutron scattering[7] show clearly two anomalies at temperatures $T_k \approx 265$ K and $T_c \approx 287$ K. This behavior shows that there must be at least three phases with different magnetic order, the high-temperature phase (HTP) for $T > T_c$ being paramagnetic. The main problem for a theory of the magnetic properties of $FeGe_2$ is to understand the nature of the intermediate-temperature phase (ITP), for $T_c > T > T_k$, and the low-temperature phase (LTP), for $T < T_k$.

The magnetic structure of the LTP was previously studied[7-12] by means of neutron diffraction in single crystals and powder samples. It was found to have a sublattice antiferromagnetic structure of moments on the Fe atoms, the crystal structure being $C16$. The moments can be projected into the basal plane, corresponding to "easy-plane" symmetry. The angle between the Fe moments in neighboring crystallographic planes was found by Forsyth *et al.*[9] to be 72°, whereas the powder diffraction work[10,11,12] found the moments to be collinear.

Sólyom and Krén[13] used Landau theory for second-order phase transitions to determine the possible types of magnetic ordering in $FeGe_2$. They postulated that the point group of the ITP should be a subgroup of the HTP and thus obtained collinear magnetic order. As temperature decreases, the magnetic ordering becomes noncollinear in the LTP if the phase transition at T_k is second order. This idea was proposed also by Krén and Szabó as in Ref. 8 and Forsyth *et al.*[9] to explain their experimental results. According to Sólyom and Krén,[13] the LTP may also have a collinear magnetic structure, but with a different symmetry from the ITP. In this case the phase transition at T_k would be first order.

Thus, over the past 20 years a picture has developed of a sequence of phases with increasing temperatures from noncollinear, through collinear, to paramagnetic, which explains the experimental results satisfactorily. However, the experiments[3] showing disappearance of the magnetic anisotropy in the basal plane are in conflict with this idea. We proposed,[14] therefore, that in the ITP the moments have a spiral structure, whose symmetry is a subgroup of the space group (but not the point group) of the HTP. Probably the formation of the incommensurate ITP is due to the Dzyaloshinski exchange mechanism,[15] the wave vector q of the spiral being determined by minimizing the exchange energy $J_1(q)\langle S\rangle^2$. The dependence of the magnitude q of the wave vector on temperature is associated with the biquadratic exchange term, $J_2(q)\langle S\rangle^4$. In this case, q is found from the minimum of the effective exchange integral, as illustrated in Fig. 1, with $J_{\text{eff}}(q)=J_1(q)+J_2(q)\langle S\rangle^2$, $\langle S\rangle$ being the average magnitude of the spin of the magnetic atom. For $T < T_k$ (case 4 in Fig. 1), $J_{\text{eff}} \sim q^2$ at small q, while for $T = T_k$ (case 3), $J_{\text{eff}} \sim q^4$.

This model for the phase transition at T_c explains the disappearance of the anisotropy in the basal plane in the

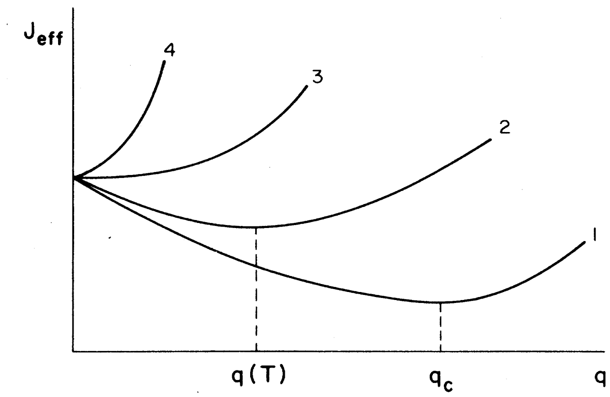

FIG. 1. Dependence of the effective exchange integral on the magnitude of the wave vector for various temperature ranges: $1-T\geq T_c$, $2-T_k<T<T_c$, $3-T=T_k$, $4-T<T_k$.

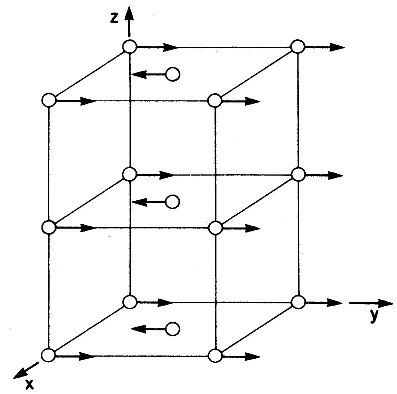

FIG. 2. Ordering of magnetic moments on the Fe atoms in the low temperature phase. The Ge atoms are not shown.

ITP. It contradicts, however, the earlier conclusions[8,9] that the LTP has noncollinear structure, since in that case there would be three phase transitions instead of two.

Corliss *et al.*[7] found by neutron diffraction a spiral structure in the ITP, with wave vector $\mathbf{q}$ along [100] or [010] and the inverse directions. The maximum value of q, $q_c a_0 \approx 0.05$, occurs at the Néel temperature T_c (referred to in Ref. 7 as T_N). As the temperature approaches the transition to the LTP at T_k (referred to in Ref. 7 as T_c), q approaches zero. Careful study of the LTP indicates collinear ordering and the interpretation of the data[8,9] is thus incorrect. The magnetic order of the Fe moments in the LTP according to Corliss *et al.*[7] is shown in Fig. 2. In the present paper we shall study the uniform state as a function of temperature and magnetic field, and deal with some questions concerning the magnetostriction in the LTP, within the framework of the Landau theory of phase transitions.

II. FREE ENERGY AND FLUCTUATION SPECTRUM

Before writing the free energy of $FeGe_2$, we take note of two important conditions. First, T_k is assumed to be close to T_c, i.e., $T_c - T_k \ll T_c$. This allows us to write the free-energy density in an expansion in ascending powers of the moments of the magnetic sublattices, $\mathbf{M}_j$ ($j=1,2,3,4$), since the $\mathbf{M}_j$ are sufficiently small. Secondly, the characteristic length of the magnitude order must be much larger than the lattice parameter a_0, so that we can use the continuous medium approximation. In this case we can write

$$\begin{aligned} F&=\int d\mathbf{r}\,F(\mathbf{r})\,, \\ F&=\tfrac{1}{2}a_{ik}\mathbf{M}_i\cdot\mathbf{M}_k+\tfrac{1}{4}b_{iklm}(\mathbf{M}_i\cdot\mathbf{M}_k)(\mathbf{M}_l\cdot\mathbf{M}_m)+\tfrac{1}{2}A_{ik}^{\alpha\beta}\nabla_\alpha\mathbf{M}_i\cdot\nabla_\beta\mathbf{M}_k+\tfrac{1}{4}B_{ik}^{\alpha\beta\gamma\delta}\nabla_\alpha\nabla_\beta\mathbf{M}_i\cdot\nabla_\gamma\nabla_\delta\mathbf{M}_k \\ &\quad+\tfrac{1}{2}C_{iklm}^{\alpha\beta}(\nabla_\alpha\mathbf{M}_i\cdot\nabla_\beta\mathbf{M}_k)(\mathbf{M}_l\cdot\mathbf{M}_m)+\tfrac{1}{2}D_{iklm}^{\alpha\beta}(\nabla_\alpha\mathbf{M}_i\cdot\mathbf{M}_k)(\nabla_\beta\mathbf{M}_l\cdot\mathbf{M}_m) \\ &\quad+\tfrac{1}{2}K_\parallel\sum_i M_{iz}^2+\tfrac{1}{4}K_\perp\sum_i(M_{ix}^4+M_{iy}^4)-\mathbf{H}\sum_i\mathbf{M}_i\,. \end{aligned} \tag{1a}$$

Here the elements of the tensor a_{ik} are of the order of magnitude of the ratio of the exchange field H_e to the moment M_0 per unit volume of the sublattice at zero temperature,

$$a\sim\frac{H_e}{M_0}\equiv\delta\sim10^3\,, \tag{1b}$$

while

$$b\sim\delta/M_0^2,\quad A\sim\delta q^2a_0^4,\quad B\sim\delta a_0^4,\quad C\sim D\sim\delta a_0^2/M_0^2\,. \tag{1c}$$

The anisotropy constants are within the limits

$$0<K_\parallel\ll\delta,\quad 0<K_\perp\ll\delta/M_0^2\,, \tag{1d}$$

and $\mathbf{H}$ is the external magnetic field.

Equation (1a) may be simplified by using the fact that the exchange interaction energy between sublattice moments is much greater than the energy associated with nonuniformity of the exchange,

$$|a\mathbf{M}^2| \gg |A(\nabla_\alpha \mathbf{M})^2| \ .$$

For fields much smaller than the exchange field, we may use an effective two-sublattice model instead of a four-sublattice model. Finally, in our analysis of the ranges of stability of the homogeneous phases we shall neglect anisotropy in the basal plane.

The equilibrium magnitudes of the magnetic moments of the four sublattices are established by the system of equations

$$dF/d\mathbf{M}_i = 0 \ .$$

For homogeneous states within this approximation, we have

$$M_T(a + bM_T^2 + \tilde{b}M_H^2) = 0 \ , \tag{2a}$$

$$H = M_H(2\chi_0^{-1} + \tilde{b}M_T^2 + \hat{b}M_H^2) \ , \tag{2b}$$

$$M_{1x} = M_{2x} = M_H, \quad M_{1y} = -M_{2y} = M_T \ .$$

Here we suppose that the magnetic field lies in the basal plane along $\hat{x}$, and we write $a = a_{11} - a_{12}$:

$$2\chi_0^{-1} = a_{11} + a_{12} \gg 1, \quad b = b_{1111} + b_{1122} + 2b_{1212} - 4b_{1112} > 0 \ ,$$

$$\tilde{b} = b_{1111} + b_{1122} - 2b_{1212} > 0, \quad \hat{b} = b_{1111} + b_{1122} + 2b_{1212} + 4b_{1112} > 0 \ .$$

Assuming as usual that $a(T)$ is a linear function of temperature, $a(T) = \alpha(T - T_0)$, we obtain the solution to the system of Eqs. (2),

$$M_T^2 = -\left[\frac{\alpha}{b}(T - T_0) + \frac{\tilde{b}}{b}M_H^2\right]\Theta[-\alpha(T - T_0) - \tilde{b}M_H^2] \ , \tag{3a}$$

$$M_H \sim \tfrac{1}{2}\chi_T H, \quad \chi_T^{-1} = \chi_0^{-1} + \tfrac{1}{2}\tilde{b}M_T^2 \ , \tag{3b}$$

$$\Theta(x) = \begin{cases} 0, & x < 0 \\ 1, & x > 0 \end{cases} .$$

We calculate the ranges of stability of the homogeneous phases by determining the spectrum of low frequency fluctuations. For this we use the Landau-Khalatnikov equations

$$\lambda \dot{\mathbf{M}}_i = -dF/d\mathbf{M}_i$$

and make the substitution,

$$\mathbf{M}_i = \mathbf{M}_{0i} + [\mathbf{M}_{si}\cos(\mathbf{k}\cdot\mathbf{r} - t/\tau)] \ .$$

We obtain the following system of equations for the characteristic lifetime τ of the fluctuations

$$(-\tau^{-1}\lambda + U_{11})M_{sx} + U_{12}L_{sy} = 0 \ , \tag{4a}$$

$$U_{12}M_{sx} + (-\tau^{-1}\lambda + U_{22})L_{sy} = 0 \ , \tag{4b}$$

and

$$(-\tau^{-1}\lambda + V_{11})M_{sy} + V_{12}L_{sx} = 0 \ , \tag{5a}$$

$$V_{12}M_{sy} + (-\tau^{-1}\lambda + V_{22})L_{sx} = 0 \ . \tag{5b}$$

Here

$$\mathbf{M}_s = \mathbf{M}_{s1} + \mathbf{M}_{s2}, \quad \mathbf{L}_s = \mathbf{M}_{s1} - \mathbf{M}_{s2} \ .$$

The nature of the vibrations described by Eqs. (4) and (5) is illustrated in Figs. 3(a) and 3(b). According to convention we name the vibration of the usual first type "longitudinal" ($\mathbf{M}_s \| \mathbf{H}$) and the second "transverse" ($\mathbf{M}_s \perp \mathbf{H}$).

It may be shown that $U_{11} \gg U_{12}, U_{22}$, and that $V_{11} \gg V_{12}, V_{22}$. Therefore, the lifetime τ_1 of the longitudinal fluctuations and τ_{tr} of the transverse may be determined in this approximation by the relations

$$\tau_1 \sim \lambda U^{-1}, \quad \tau_{tr} \sim \lambda V^{-1} \ , \tag{6}$$

where

$$U \equiv U_{22}(\mathbf{k}) = a + \tilde{b}M_H^2 + 3bM_T^2 + \mathbf{k}[-\hat{A} + \tilde{C}M_H^2 + (\hat{C} + \hat{D})M_T^2]\mathbf{k} + \tfrac{1}{2}\mathbf{k}\cdot\mathbf{k}\cdot\hat{B}\cdot\mathbf{k}\cdot\mathbf{k} \ , \tag{7a}$$

$$V \equiv a + (2\tilde{b}_0 + \tilde{b})M_H^2 + bM_T^2 + \mathbf{k}[-\hat{A} + (\tilde{C} + \tilde{D})M_H^2 + \hat{C}M_T^2]\mathbf{k} + \tfrac{1}{2}\mathbf{k}\cdot\mathbf{k}\cdot\hat{B}\cdot\mathbf{k}\cdot\mathbf{k} \ , \tag{7b}$$

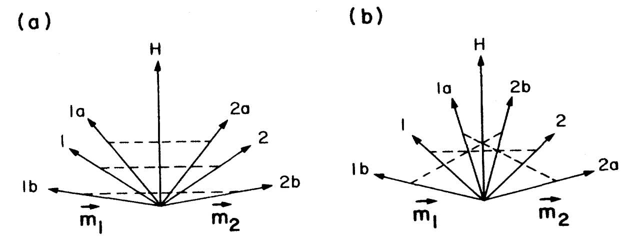

FIG. 3. Illustration showing the vibrations for longitudinal (a) and transverse (b) fluctuations.

and

$$\hat{C}=\hat{C}_{1111}+\hat{C}_{1122}+\hat{C}_{1212}-\hat{C}_{1112}-2\hat{C}_{1211}\ ,$$
$$\tilde{C}=\tilde{C}_{1111}+\tilde{C}_{1122}+\tilde{C}_{1112}-\tilde{C}_{1212}-2\tilde{C}_{1211}\ ,$$

$$\hat{D}=\hat{D}_{1111}+\hat{D}_{1122}+\hat{D}_{1212}+\hat{D}_{1221}-2\hat{D}_{1112}-2\hat{D}_{1121}\ ,$$
$$\tilde{D}=\hat{D}_{1111}+\hat{D}_{1212}+2\hat{D}_{1112}-\hat{D}_{1122}-\hat{D}_{1221}-2\hat{D}_{1121}\ , \tag{8}$$

$$\hat{A}=\hat{A}_{12}-\hat{A}_{11},\quad \hat{B}=\hat{B}_{11}-\hat{B}_{12},\quad \tilde{b}_0=b_{1111}-b_{1122}>0\ .$$

III. RANGES OF STABILITY OF THE HOMOGENEOUS PHASES

We shall evaluate first the phase boundary of the paramagnetic state. For this purpose we put $M_T=0$ in both expressions (7a) and (7b). The magnitude of k is small, with $\tilde{C}k^2 \ll \tilde{b}$, and $\tilde{b}_0>0$, so that for the paramagnetic phase, $U<V$. Consequently stable equilibrium of the paramagnetic phase is determined by the inequality

$$U=a+\tilde{b}M_H^2+(-A_\perp+\tilde{C}_\perp M_H^2)k_\perp^2+(-A_\parallel+\tilde{C}_\parallel M_H^2)k_z^2 +\tfrac{1}{2}B_1(k_x^4+k_y^4)+\tfrac{1}{2}B_3k_z^4 +3B_2k_x^2k_y^2+3B_4(k_x^2+k_y^2)k_z^2>0\ . \tag{9}$$

In accordance with the experimental data,[7] we write $A_\perp > A_\parallel$, $A_\perp>0$, $B_3>B_1>0$, and $3B_2>B_1$. By determining the minimum of $U(\mathbf{k})$, we obtain the stability criterion for the paramagnetic phase

$$a\equiv\alpha(T-T_0)\ge -\tfrac{1}{4}\tilde{b}\chi_0^2H^2+\frac{1}{2B_1}(A_\perp-\tfrac{1}{4}\tilde{C}_\perp\chi_0^2H^2)^2 \times\theta(A_\perp-\tfrac{1}{4}\tilde{C}_\perp\chi_0^2H^2) \tag{10}$$

with $M_H\simeq\frac{1}{2}\chi_0 H$ from (3) since $M_T=0$.

The relation between the transition temperature T_c and the characteristic temperature T_0 may be obtained from Eq. (10) with $H=0$

$$a_c\equiv\alpha(T_c-T_0)=A_\perp{}^2/2B_1\equiv\tfrac{1}{2}B_1q_c^4\sim\delta(a_0q_c)^4\ . \tag{11a}$$

The phase boundary near T_c is of the form

$$T_c-T=a_2H^2-a_4H^4,\quad \text{with } a_2,\ a_4>0\ . \tag{11b}$$

The other characteristic temperature, the tricritical point (H_t,T_t), may be calculated by the condition that the second-order derivative d^2T/dH^2 develops a discontinuity, giving

$$a_t\equiv\alpha(T_t-T_0)=-\tfrac{1}{4}\tilde{b}\chi_0^2H_t^2\sim-\delta(a_0q_c)^2\ , \tag{12a}$$

$$H_t=2\chi_0^{-1}(A_\perp/\tilde{C}_\perp)^{1/2}\sim H_e a_0 q_c\ . \tag{12b}$$

The region of existence of the low-temperature homogeneous antiferromagnetic phase is determined by the system of inequalities

$$U(k)=2bM_T^2+[-A_\perp+\tilde{C}_\perp M_H^2 +(C_\perp+D_\perp)M_T^2]k^2+\tfrac{1}{2}B_1k^4\ge 0\ , \tag{13a}$$

$$V(k)=2\tilde{b}_0M_H^2+[-A_\perp+(\tilde{C}_\perp+\tilde{D}_\perp)M_H^2 +C_\perp M_T^2]k^2+\tfrac{1}{2}B_1k^4\ge 0\ , \tag{13b}$$

where

$$M_T^2=-\frac{a+\tilde{b}M_H^2}{b}\approx-\frac{a+\frac{1}{4}\tilde{b}\chi_0^2H^2}{b}>0$$

and

$$H=M_H[2\chi_0^{-1}-a\tilde{b}/b+(\hat{b}+\tilde{b}^2/b)M_H^2]\approx 2\chi_0^{-1}M_H\ .$$

Analysis of Eqs. (13) shows that, for relatively weak magnetic fields ($H<H_p$) near the boundary of the antiferromagnetic region, the transverse fluctuations grow with the field. For stronger fields, instability of the boundary is manifested by the growth of longitudinal fluctuations. The coordinates of the critical point (H_p,T_p) are solutions of the system of equations

$$U(k_1)=0,\quad V(k_2)=0,\quad U'(k_1)=0,\quad V'(k_2)=0$$

under the condition $U''(k_1)$, $V''(k_2)>0$. From this we have,

$$a_p\equiv\alpha(T_p-T_0)\approx-\tfrac{1}{4}\tilde{b}\chi_0^2H_p^2\sim\delta(a_0q_c)^4\ , \tag{14a}$$

$$H_p=\chi_0^{-1}q_c^2\sqrt{B_1/\tilde{b}_0}\sim H_e(a_0q_c)^2\ . \tag{14b}$$

The final expressions, which determine the stability of the phase boundaries, then have the appearance, if $H<H_p$,

$$a\equiv\alpha(T-T_0)<-\frac{\tilde{b}\chi_0^2H^2}{4}-\frac{b}{C_\perp}[A_\perp-\tfrac{1}{4}(\tilde{C}_\perp+\tilde{D}_\perp)\chi_0^2H^2 -\chi_0H(\tilde{b}_0B_1)^{1/2}] \tag{15}$$

and, if $H_p<H$,

$$a\equiv\alpha(T-T_0)<-\frac{\tilde{b}\chi_0^2H^2}{4}-\frac{b}{4\tilde{b}B_1}(A_\perp-\tfrac{1}{4}\tilde{C}_\perp\chi_0^2H^2)^2 \times\theta(A_\perp-\tfrac{1}{4}\tilde{C}_\perp\chi_0^2H^2)\ . \tag{16}$$

From Eq. (16) it may be seen that the antiferromagnetic phase boundaries coincide with the stability boundaries of the paramagnetic phase into the tricritical point t, as shown in Fig. 4. The relation between T_k and T_0 may be obtained from Eq. (15) by setting $H=0$,

$$a_k\equiv\alpha(T_k-T_0)=-\frac{b}{C_\perp}A_\perp=-\frac{b}{C_\perp}B_1q_c^2\sim-\delta(a_0q_c)^2\ . \tag{17}$$

The boundaries of the homogeneous magnetic phases and the critical points are shown schematically in the field-temperature phase diagram of Fig. 4.

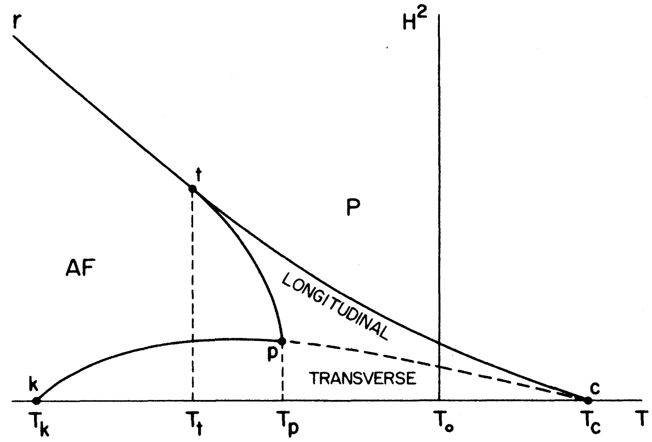

FIG. 4. Schematic phase diagram showing the homogeneous states and phase boundaries in $FeGe_2$. The line *rt* corresponds to a second-order phase transition from the homogeneous antiferromagnetic phase to the paramagnetic phase. The point *t* is a tricritical point. The line *tc* corresponds to the transition boundary from the paramagnetic phase to the longitudinal spiral structure, while the line *tp* is the boundary for transition from the homogeneous antiferromagnetic phase. Line *kp* is the boundary between the homogeneous antiferromagnetic phase and the transverse spiral structure. Line *pc* (not calculated) must correspond to a first-order transition from one type of spiral structure to another.

IV. MAGNETIC STRUCTURE OF THE INTERMEDIATE PHASE IN ZERO FIELD

In the previous section we found that for a small magnetic field the antiferromagnetic phase is unstable to formation of a transverse spiral structure. Consequently, for $H=0$ and $T_k < T < T_c$, we shall look for solutions of equations of the form

$$\mathbf{M}_{1,2} = \pm M[\mathbf{e}_x \cos(\mathbf{q}\cdot\mathbf{r} + \mathbf{e}_y)\sin(\mathbf{q}\cdot\mathbf{r})] \ . \tag{18}$$

The spiral wave vector $\mathbf{q}$ and magnetization amplitude M are chosen to minimize the free energy,

$$\begin{aligned} F &= aM^2 + \tfrac{1}{2}bM^4 + (-A_\perp + C_\perp M^2)M^2(q_x^2+q_y^2) \\ &\quad + (-A_\parallel + C_\parallel M^2)M^2 q\frac{2}{z} + \frac{1}{2}B_1(q_x^4+q_y^4)M^2 \\ &\quad + \tfrac{1}{2}B_3 q_z^4 M^2 + 3B_2 q_x^2 q_y^2 M^2 + 3B_4 M^2 q_z^2(q_x^2+q_y^2) \ , \end{aligned} \tag{19}$$

which is obtained by substituting Eq. (18) into Eq. (1).

The vector $\mathbf{q}$ is directed either along $\hat{x}$ or $\hat{y}$ according to experiment.[7] This means that the following inequalities obtain: $A_\perp > A_\parallel$, $B_1 < B_3$, $3B_2$. Suppose $\mathbf{q}$ is along $\hat{x}$, then it follows from the equations

$$\frac{\partial F}{\partial M} = 2M(a + bM^2 - A_\perp q^2 + \tfrac{1}{2}B_1 q^4 + 2C_\perp q^2 M^2) = 0 \ , \tag{20a}$$

$$\frac{\partial F}{\partial q} = 2qM^2(-A_\perp + B_1 q^2 + C_\perp M^2) = 0 \tag{20b}$$

that there exist three phases: (a) paramagnetic phase for $M=0$; (b) antiferromagnetic phase for $q=0$, $M^2 = -a/b > 0$; and (c) incommensurate phase for $q \neq 0$ and $M \neq 0$.

The stable boundary of the paramagnetic phase is determined by the inequality

$$\frac{\partial^2 F}{\partial M^2} = 2(a - A_\perp q^2 + \tfrac{1}{2}B_1 q^4) \geq 0 \ ,$$

which is equivalent to the expression

$$a \equiv \alpha(T - T_0) \geq a_c = A_\perp^2/2B_1 = \tfrac{1}{2}B_1 q_c^4 \tag{21}$$

corresponding to $T \geq T_c$ and $H=0$ in accordance with Eq. (10). The inequality

$$\partial^2 F/\partial q^2 = 2M^2(-A_\perp + C_\perp M^2) \geq 0$$

determines the stable boundary of the antiferromagnetic phase. This is equivalent to the inequality

$$a \leq a_k = -\frac{b}{C_\perp} A_\perp \tag{22}$$

corresponding to $T \leq T_k$ and $H=0$.

We shall now examine in more detail the properties of the incommensurate phase. The solution of Eq. (20) gives us the magnitude of both the spiral wave vector $\mathbf{q}$ and the magnetization M of the sublattice as functions of temperature

$$q^2/q_c^2 = \frac{1}{6}\left\{ \left[\left[\frac{3T_0 - T_k - 2T_c}{T_c - T_0} \right]^2 + 12\frac{T - T_k}{T_c - T_0} \right]^{1/2} - \frac{3T_0 - T_k - 2T_c}{T_c - T_0} \right\} , \tag{23}$$

$$M^2(T) = \frac{A_\perp}{C_\perp}(1 - q^2/q_c^2) \tag{24}$$

with $q_c^2 \sim A_\perp / B_\perp$ from Eq. (1c). It may be seen that $q(T)$ increases monotonically with temperature from $q=0$ $(T=T_k)$ up to $q=q_c$ $(T=T_c)$. The rate of increase $\partial q(T)/\partial T$ slowly decreases with temperature increasing, in agreement with the experimental data of Corliss *et al.* shown in Fig. 5 of Ref. 7 (note that in this paper the

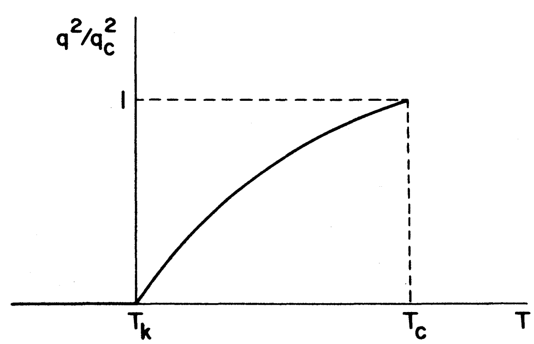

FIG. 5. Temperature dependence of the wave vector in the transverse spiral phase (schematic).

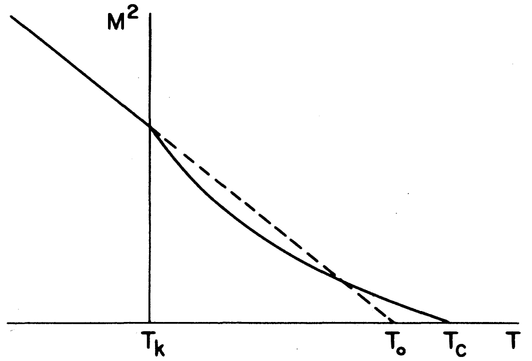

FIG. 6. Temperature dependence of the sublattice moment (schematic).

lower transition is denoted T_c and the upper T_N). In Figs. 5 and 6 we show schematically $(q/q_c)^2$ and M^2 as functions of temperature.

Analysis of the solutions (23) and (24) for stability show that the free energy F is a minimum in the range $T_k < T < T_c$. Thermodynamic analysis shows that the entropy is continuous at T_k and at T_c, but the heat capacity is discontinuous at each temperature. This is normal for a second-order phase transition. If we take into account planar magnetic anisotropy, we obtain an equation of state for an incommensurate phase analogous to that produced by an external magnetic field. Therefore, magnetic anisotropy in the basal plane can change the character of the transition at T_k to weak first order. At the same time, this anisotropy does not greatly influence T_c, since the anisotropy energy near T_c approaches zero as M^4. Pluzhnikov *et al.*[5] have indeed found the lower-temperature transition to be hysteretic under thermal and stress cycling.

V. MAGNETIZATION AND MAGNETOSTRICTION: EFFECT OF CRYSTAL INHOMOGENEITY

The present section will deal specifically with interpretation of the experimental data[6] for the magnetostriction as a function of temperature and magnetic field. First we shall discuss the process of magnetization of the low-temperature antiferromagnetic phase, where the magnetostriction experiments were performed. Let us suppose that the crystal is slightly imperfect and that it consists of microscopically small domains, whose size is much larger than the width of the domain boundary. In each domain the tetragonal symmetry is slightly distorted, and one of the two formerly equivalent directions in the basal plane will be preferred. We shall describe this situation in terms of small random uniaxial anisotropy in the basal plane, so that the magnetic part of the free-energy density in the two-sublattice model may be written

$$F_M = J\mathbf{M}_1\cdot\mathbf{M}_2 + \tfrac{1}{2}\beta_u(M_{1z}^2 + M_{2z}^2) - \frac{\beta}{4M^2}(M_{1x}^4 + M_{1y}^4 + M_{2x}^4 + M_{2y}^4) - \tfrac{1}{2}\tilde{\beta}(\mathbf{r})(M_{1x}^2 + M_{2x}^2) - (\mathbf{M}_1 + \mathbf{M}_2)\cdot\mathbf{H} \; , \tag{25}$$

where J is the exchange constant, β_u is the uniaxial anisotropy constant, β is the anisotropy constant in the basal plane ($\beta_u > 0$, $\beta > 0$), $\tilde{\beta}(\mathbf{r})$ is the random anisotropy within the region $\mathbf{r}$, and $F = \int F(\mathbf{r})d\mathbf{r}$.

Let the field $\mathbf{H}$ in the basal plane make an angle ψ with $\hat{x}$ and denote the angle between the magnetic moments by $\pi - \omega$, and the angle between the resultant moment and $\hat{x}$ by ϕ. Equation (25) then becomes

$$F_M = M^2\left[-J + \frac{1}{2}\tilde{\beta}\cos 2\phi\cos 2\omega - \frac{\beta}{8}\cos 4\phi\cos 4\omega - 2h\sin\omega\cos(\phi-\psi)\right] , \tag{26}$$

where $h = H/M$.

Minimizing Eq. (26) with respect to ω, keeping in mind that $J \gg \beta \gg \tilde{\beta}$, we obtain

$$M^{-2}F_M = -\tfrac{1}{8}\beta\cos 4\phi + \tfrac{1}{2}\tilde{\beta}\cos^2\phi - \frac{h^2}{4J}\cos^2(\phi-\psi) \; . \tag{27}$$

We can see that in the absence of magnetic field the random anisotropy selects a preferred direction for the antiferromagnetic wave vector, $\mathbf{L} = \mathbf{M}_1 - \mathbf{M}_2$. Hence, if $\tilde{\beta} > 0$, then $\phi = \pi/2$ and $\mathbf{L}\|\hat{x}$. Otherwise, if $\tilde{\beta} < 0$, then $\phi = 0$ and $\mathbf{L}\|\hat{y}$.

Supposing that $\psi < \pi/4$, and keeping in mind that in a magnetic field the disappearance of domains of unfavorable orientation takes place through motion of the domain boundary, we see that the domain develops a magnetic moment if

$$\tilde{\beta} - \frac{h^2}{2J}\cos 2\psi < 0 \tag{28}$$

and remains unmagnetized otherwise. We now evaluate the concentration of phase $c(H)$ of the phase for which the orientation of the antiferromagnetic vector is $\mathbf{L}\|\hat{y}$, by assuming a Gaussian distribution for $\tilde{\beta}(\mathbf{r})$

$$\begin{aligned} c(H) &= \frac{I}{\sqrt{\pi}\beta_0}\int_{-\infty}^{+\infty} d\tilde{\beta}\exp(-\tilde{\beta}^2/\beta_0^2)\Theta\left[\frac{h^2}{2J} - \tilde{\beta}\right] \\ &= \frac{1}{\sqrt{\pi}}\int_{-\infty}^{H^2\cos 2\psi/H_0^2} dx\,\exp(-x^2) \\ &= \tfrac{1}{2}[1 + \Phi(H^2\cos 2\psi/H_0^2)] \; . \end{aligned} \tag{29}$$

Here $H_0 = M(2J\beta_0)^{1/2}$, $\Theta(x)$ is the step function defined in Eq. (3), and $\Phi(x)$ is the probability integral. For the case of small magnetic fields, $H \ll H_0$,

$$c(H) \approx \frac{1}{2} + \frac{H^2}{\sqrt{\pi}H_0^2}\cos 2\psi \; .$$

In strong fields much greater than the characteristic field H_0, $1 - c(H) \sim 0$. If $\psi = \pi/4$, then $c = \frac{1}{2}$.

From this point of view we consider the magnetostriction experiment.[6] We denote the diagonal elements of the deformation tensor for the preferred orientation corresponding to a given field direction by u_{xx}, u_{yy}, and u_{zz} and we obtain for the unfavorable phase the following distribution of deformations among the axes, u_{yy}, u_{xx}, and u_{zz}. Then the deformations ϵ_k found by experiment, expressed in terms of the random deformations u_{ik}, have the form

$$\begin{aligned} \epsilon_{xx} &= cu_{xx}+(1-c)u_{yy}-\tfrac{1}{2}(u_{xx}+u_{yy}) \\ &= (c-\tfrac{1}{2})(u_{xx}-u_{yy})=\epsilon_0(2c-1) , \\ \epsilon_{yy} &= -(c-\tfrac{1}{2})(u_{xx}-u_{yy})=-\epsilon_{xx} , \\ \epsilon_{zz} &= 0 , \end{aligned} \tag{30}$$

and

$$\epsilon_0=\tfrac{1}{2}(u_{xx}-u_{yy}) .$$

The magnetostriction illustrated schematically in Fig. 7 compares well with the experimental dâta of Franus-Muir *et al.* shown in Fig. 1 of Ref 6.

Finally, we determine the form of the temperature dependence of the deformation ϵ_0 and of the characteristic field H_0. The energy of magnetostriction F_M and elastic energy F_E are written

$$\begin{aligned} F_M &= \Gamma^{ik}_{\alpha\beta\gamma\delta}M_i^\alpha M_k^\beta u_{\gamma\delta} , \\ F_E &= \tfrac{1}{2}c_{11}(u_{xx}^2+u_{yy}^2)+\tfrac{1}{2}c_{33}u_{zz}^2+c_{12}u_{xx}u_{yy} \\ &\quad +c_{13}u_{zz}(u_{xx}+u_{yy})+2c_{66}u_{xy}^2+2c_{44}(u_{xz}^2+u_{yz}^2) . \end{aligned} \tag{31}$$

Here $\hat{\Gamma}$ is the magnetostriction constant tensor, and c_{ik} are the elastic moduli; the Greek indices denote Cartesian coordinate axes and the Latin indices the magnetic sublattice axes. If the domains are sufficiently large then the u_{ik} may be determined from the condition $\sigma_{ik} \equiv \partial F/\partial u_{ik}=0$. Solving this system of equations, we obtain

$$\epsilon_0=\tfrac{1}{2}(u_{xx}-u_{yy})=\frac{\Gamma_{11}^{ik}-\Gamma_{12}^{ik}}{2(c_{11}-c_{12})}M_i^\gamma M_k^\gamma , \tag{32}$$

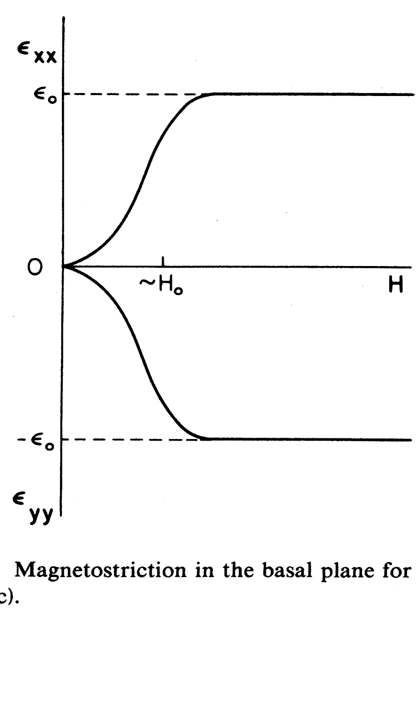

FIG. 7. Magnetostriction in the basal plane for field along $\hat{x}$ (schematic).

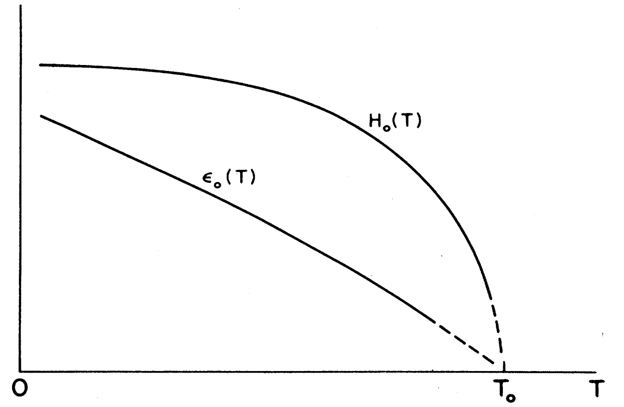

FIG. 8. Temperature dependence of the deformation ϵ_0 and the characteristic field H_0 (schematic).

where $\Gamma_{11}=\Gamma_{xxxx}$, $\Gamma_{12}=\Gamma_{xxyy}$. From Eq. (32) we see that ϵ_0 varies like M^2 and thus ϵ_0 decreases almost linearly as temperature increases. At the same time $H_0 \sim M \sim (T_0-T)^{1/2}$. The temperature dependence of ϵ_0 and H_0 illustrated in Fig. 8 is similar to that found by Franus-Muir *et al.* and shown in Fig. 3 of Ref. 6.

VI. DISCUSSION

We can very roughly estimate the exchange field H_e from the low-temperature value m_0 of the magnetic moment per Fe atom, $m_0=1.2\mu_B$,[8–12] and the Néel temperature, $T_N \equiv T_c \simeq 287$ K, by employing the formula

$$H_e \simeq \frac{k_B T_N}{m_0} \sim 3\times10^8 Am^{-1} \tag{33a}$$

or

$$B_e=\mu_0 H_e \sim 400 \text{ T} . \tag{33b}$$

The use of an effective two-sublattice instead of a four-sublattice model is justified by this large value for the exchange field. The number per unit volume of Fe atoms, $N=2.3\times10^{28}$ m^{-3}, gives a moment per unit volume of the sublattice

$$M_0=Nm_0=2.6\times10^5 Am^{-1} \tag{34}$$

so that $\delta \equiv H_e/M_0 \sim 10^3$, as given in Eq. (1c).

From H_e we can estimate the tricritical field H_t and the critical field H_p, by use of the approximations (12b) and (14b), respectively, and the value, $a_0q_c \simeq 0.05$, for the wave vector of the spiral structure close to these critical temperatures. The resultant values for the magnetic induction at these critical points are

$$B_t=\mu_0 H_t \sim \mu_0 H_e a_0 q_c \sim 20 \text{ T} , \tag{35a}$$

$$B_r=\mu_0 H_r \sim \mu_0 H_0 (a_0 q_c)^2 \sim 1 \text{ T} . \tag{35b}$$

These values suggest that the interesting region of the phase diagram in the neighborhood of the line *kpc* in Fig. 4, where these transverse spiral structure changes into the longitudinal spiral structure or into the antiferromagnetic structure, could be explored with quite modest magnetic fields. A considerably larger field would be required to explore the neighborhood of the tricritical point.

Unfortunately the large value of the exchange field H_e makes the field dependence of the Néel temperature T_c very weak, while the small value of the wave vector $a_0 q_c$ makes the range of temperatures over which the longitudinal spiral phase exists very narrow. Thus Eqs. (11a), (14a), and (17) give

$$\Delta T_c = |T_0 - T_c| \sim (\delta/\alpha)(a_0 q_c)^4 ,$$

$$\Delta T_p = |T_0 - T_p| \sim (\delta/\alpha)(a_0 q_c)^4 ,$$

$$\Delta T_k = |T_0 - T_k| \sim (\delta/\alpha)(a_0 q_c)^2 ,$$

and, with $a_0 qc \simeq 0.05$, we find that

$$|\Delta T_c| \sim |\Delta T_p| \sim |\Delta T_k| (a_0 q_c)^2 \sim 10^{-3} |\Delta T_k|$$

so that

$$|\Delta T_k| \simeq (\Delta T)_0 = T_c - T_k \simeq 22 \text{ K}$$

and

$$T_c - T_p \simeq \Delta T_p \sim 10^{-3} (\Delta T)_0 \simeq 20 \text{ mK} . \tag{36}$$

An estimate can similarly be obtained for the slope, $\Delta T / H^2 = (T_c - T)/H^2$, of the paramagnetic phase boundary from the experimental value of $(\Delta T)_0$ and Eq. (10), which gives

$$\frac{\Delta T}{(\Delta T)_0} \sim \left[\frac{H}{H_e} \right]^2 . \tag{37a}$$

Thus, for $B = \mu_0 H = 10$ T, a quite large magnetic induction, we obtain

$$\Delta T \sim 20 \text{ mK} . \tag{37b}$$

The effect of a magnetic field is so small because the high Néel temperature, $T_N \equiv T_c$, and large exchange field H_e go together, according to Eq. (33a). The field dependence in Cr, with $T_N = 312$ K, is very weak for the same reason, with a magnetic induction, $B = 16$ T, producing no change in T_N greater than $+10$ mK or -20 mK.[16]

Since the resolution of the temperature of the Néel transition in the best available samples is only about 0.5 K (see Fig. 1 of Ref. 5) and Figs. 5 and 9 of Ref. 7), these small values of $T_c - T_p$ and $\Delta T(H)$ make an experimental study of these features of the phase diagram unattractive. On the other hand, the relatively small value of the critical field H_p given by Eq. (35b), and the fact that the field at which the transition occurs from the transverse spiral phase to the antiferromagnetic phase decreases monotonically from T_p to Tk, as shown in Fig. 4, makes this feature a promising candidate for an experimental study.

We are planning a study of the magnetostriction and the field dependence of the ultrasonic velocity and attenuation in the intermediate phase between T_k and T_c, in order to locate the transition from the transverse spiral phase to the antiferromagnetic phase. If we are successful, a neutron diffraction study will follow.

ACKNOWLEDGMENTS

This work was supported by the Natural Sciences and Engineering Research Council of Canada. Two of the authors (V.V.T. and V.P.) wish to acknowledge the hospitality of Department of Physics, University of Toronto.

[1]R. P. Krentsis, A. V. Mikhl'son, and P. V. Gel'd, Fiz. Tverd Tela (Leningrad) **12**, 933 (1970) [Sov. Phys.—Solid State **12**, 727 (1970)].

[2]A. V. Mikhel'son, R. P. Krentsis, and P. V. Gel'd, Fiz. Tverd. Tela (Leningrad) **12**, 2470 (1970) [Sov. Phys.—Solid State **12**, 1979 (1971)].

[3]J. J. Piritinskaya, A. V. Mikhel'son, and R. P. Krentsis, Fiz. Tverd. Tela (Leningrad) **21**, 1833 (1979) [Sov. Phys.—Solid State **21**, 1050 (1979)].

[4]G. P. Zinov'eva, A. V. Mikhel'son, L. P. Andreeva, R. P. Krentsis, and P. V. Gel'd, Fiz. Tverd. Tela (Leningrad) **14**, 1578 (1972) [Sov. Phys.—Solid State **14**, 1364 (1972)].

[5]V. Pluzhnikov, D. Feder, and E. Fawcett, J. Magn. Magn. Mater. **27**, 343 (1982).

[6]E. Franus-Muir, E. Fawcett, and V. Pluzhnikov, Solid State Commun. **52**, 615 (1984).

[7]L. M. Corliss, J. M. Hastings, W. Kunnmann, R. Thomas, J. Zhuang, R. Butera, and D. Mukamel, Phys. Rev. B **31**, 4337 (1985).

[8]E. Krén and P. Szabó, Phys. Lett. **11**, 215 (1964).

[9]J. B. Forsyth, C. E. Johnson, and P. J. Brown, Philos. Mag. **10**, 713 (1964).

[10]N. S. Satya Murthy, R. J. Begum, C. S. Somanathan, and M. R. L. N. Murthy, Solid State Commun. **3**, 113 (1965).

[11]E. F. Bertaut and J. Chenevas, Solid State Commun. **3**, 117 (1965).

[12]E. Adelson and A. E. Austin, Bull. Am. Phys. Soc. **10**, 352 (1965); J. Phys. Chem. Solids **26**, 1795 (1965).

[13]J. Sólyom and E. Krén, Solid State Commun. **4**, 255 (1966).

[14]E. Fawcett, V. B. Pluzhnikov, and V. V. Tarasenko, Digests XVII All Union Conf. Phys. Magn. Phenom. USSSR **1**, 99 (1985) (in Russian).

[15]I. E. Dzyaloshinski, J. Phys. Chem. Solids **4**, 241 (1958).

[16]Z. Barak, E. Fawcett, D. Feder, G. Lorincz, and M. B. Walker, J. Phys. F **11**, 915 (1981).